IEEE Access
Multidisciplinary ⋮ Rapid Review ⋮ Open Access Journal

Received October 15, 2020, accepted November 2, 2020, date of publication November 11, 2020,
date of current version November 23, 2020.

*Digital Object Identifier 10.1109/ACCESS.2020.3037364*

# Analysis of Quantum Radar Cross-Section by Canonical Quantization Method (Full Quantum Theory)

**AHMAD SALMANOGLI[1,2] AND DINCER GOKCEN[1], (Member, IEEE)**
[1]Department of Electrical and Electronics Engineering, Faculty of Engineering, Hacettepe University, 06800 Ankara, Turkey
[2]Department of Electrical and Electronics Engineering, Faculty of Engineering, Çankaya University, 06790 Ankara, Turkey

Corresponding author: Dincer Gokcen (dgokcen@hacettepe.edu.tr)

**ABSTRACT** This article investigates the difference between two quantum-based theories to calculate the radar cross-section (RCS). Quantum radar cross-section (QRCS) has been commonly analyzed using the dipole approximation method, and the related results show that it can improve the sidelobe of the interference pattern in contrast to the classical methods. This study, on the other hand, utilizes the canonical quantization (or microscopic) method, which is a more comprehensive theory than the dipole approximation method to calculate the radar cross-section. It is shown that there are some similarities between two methods; nonetheless, there are some crucial quantities and factors that have been ignored in the dipole approximation methods. The main difference arises due to the interaction Hamiltonian that two methods relied on. The theoretical calculation shows some critical points suggesting that the dipole approximation method cannot cover all aspects of the radar cross-section calculation. To verify the mentioned point, we establish a new method in which the radar cross-section is calculated by merging the quantum approach with the method of moment (MoM), called quantum-method of moment (QMoM). The simulation results show that the newly established method is in harmony with the canonical quantization method.

**INDEX TERMS** Radar cross-section, quantum radar cross-section, canonical quantization method, method of moment.

## I. INTRODUCTION

Radar cross-section (RCS) predicting an arbitrarily shaped target is one of the crucial tasks that have been studied by different exact and numerical methods [1]–[4]. The mentioned methods utilize the classical picture to calculate RCS and are known as classical RCS (CRCS). The classical theory defines the RCS based on the induced current on the target to generate the scattering electromagnetic fields [4], [5]. RCS is the ability of the target to backscatter the intercepted radar signal and fundamentally depends on the projected cross-section, as well as reflectivity and directivity of the target [6]. This means that RCS is not the projected geometric area. More technically, RCS is a function of the position of radar's transmitter and receiver relative to the target, target geometry and composition, incident wave frequency, transmitter, and receiver polarization [7], [8].

The associate editor coordinating the review of this manuscript and approving it for publication was Wei Huang.

To accurately analyze the RCS, recently, the trend has been concentrated on the quantum-based approach (quantum electrodynamics theory) utilizing quantum radar [9]–[13] to improve the radar cross-section calculation. The RCS calculated via the quantum phenomena is called quantum RCS (QRCS). This technique can be used by quantum radar [9], [11]. Quantum radar is a sensing device utilizing quantum illumination protocol [9] to enhance the system performance, such as signal-to-noise ratio and detection of the target in a noisy medium. In quantum radar, two entangled photons (signal and idler) are generated through which signal mode is propagated toward the target, and simultaneously the idler is kept in the laboratory. Eventually, the entanglement between retained (idler) and returned signals (propagated and reflected fields from target) is evaluated.

There is an essential difference between the calculation of CRCS and QRCS. QRCS describes the interaction between the intercepted photons' field and atoms of the target through the dipole approximation method [9], [10].

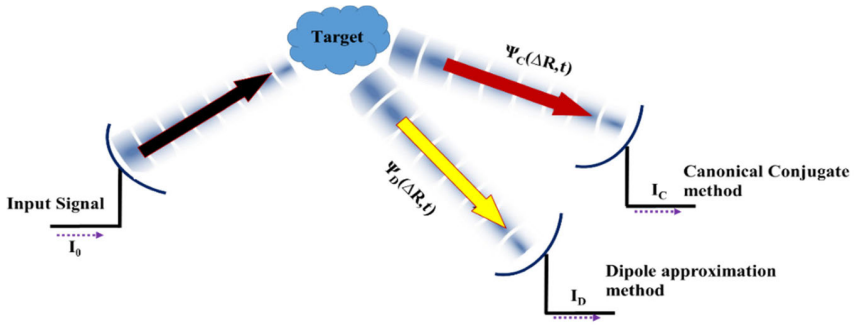


**FIGURE 1.** System schematic in which the target is incident by the broadcasting photons, and the detected signals are analyzed by two different methods at the same place in the same conditions.

Moreover, it should be noted that in QRCS, the diffraction and absorption effect is usually ignored [5] through which the calculation accuracy can be decreased. Previous studies discussed why QRCS enhances sidelobes over CRCS [12], [13]. It is theoretically proved that the QRCS equation contains a term $|\cos(\theta)|$ ($\theta$ is the incident angle) [12], whereas the CRCS equation includes a term $\cos^2(\theta)$ [12], [13]. The origin of the term $\cos^2(\theta)$ in the CRCS equation comes from the decomposition of the induced current density on the target. The results simulated in [5], [12], [13] shows that QRCS improves the RCS in the sidelobe.

Nonetheless, one can claim that QRCS may be an incomplete method because it uses an approximation based method to calculate RCS. Here, in this study, we want to answer some critical questions about it: Is the dipole approximation a perfect method to analyze RCS? Can we develop another method to improve the QRCS? To answer the questions mentioned above, here, we prefer to utilize the canonical quantization methods [11], [17], rather than the dipole approximation. It is known that this theory covers a full interaction between the incident field and the atom's field. Using this method, we derive the scattering photons wave function and compare the results with the wave functions of photons derived with the dipole approximation method [12], [13]. It is found that there are some crucial differences between the two methods, which suggests that the canonical quantization method can improve the RCS. To prove this point, additionally, we establish a new method in which we merge the quantum theory to the method of moment (MoM) [3], [14] to calculate the RCS.

RCS prediction for an arbitrarily shaped perfect conductor (PEC) through MoM has been recently investigated [3], [14]. In MoM, the electric field integral equation in which the total tangential electric field on the PEC surface is set to be zero is solved. Initially, the PEC surface is divided into rectangular or triangular subdomains, and by choosing suitable basis and weighting functions, the integral equation is reduced to a matrix equation. One can calculate the scattering field after solving the matrix equation for unknown coefficients, which leads to the calculation of the current density in RCS problems [15]. The RCS is figured out using the surface current. In contrast with the classical MoM, we establish a new method utilizing MoM with the current density operator (QMoM) to calculate the scattering field and RCS. Using the current density operator [16], [17] gives us some degrees of freedom, while it was ignored when the classical theory employs the current density average. The results indicate that QMoM predicts the enhancement of sidelobes, which confirms the achievement of QRCS. Also, it reveals an enhancement in the main lobe, and that point has not ever been predicted by QRCS calculation. This key point confirms the difference between the canonical quantization and dipole approximation methods that we want to discuss in detail in the following.

The novelty of this study can be shortly summarized as: (I) Using canonical quantization method as a complete quantum theory to enhance the RCS calculation; (II) Showing the point that the dipole approximation method is incomplete to analyze RCS; (III) Establishing a new numerical method called QMoM to calculate RCS.

The present work organization is as follows: In section II and part A, the theory and background of the study are presented, and in this part, we try to theoretically prove the difference between two quantum-based methods to calculate the emitted photons wave function. Also, in section II and part B, the new MoM based algorithm called QMoM is presented. In this part, all of the associated formula derived for MoM will be re-derived for QMoM. In section III, the simulation results will be presented, and finally, in section IV, we offer a short conclusion.

## II. THEORY AND BACKGROUND

In this section, RCS calculations through two different quantum-based methods, dipole approximation and canonical quantization methods, are examined and compared with each other. For this reason, we initially suggest considering the schematic of the system illustrated in Fig. 1. It is supposed that a wave with an intensity of $I_0$ propagates into the atmosphere to the incident upon a target, and the scattering signals are detected by two similar detectors at the same place. The detecting signals are analyzed via two different approaches to compare the results. In the following, we focus on the canonical quantization method and theoretically derive $\Psi_c(\Delta R,t)$, which is the wave function of the scattering photons, and compare with $\Psi_D(\Delta R,t)$, which has been derived by the dipole approximation method [12], [13].

### A. CANONICAL QUANTIZATION METHOD TO DERIVE THE SCATTERING PHOTONS WAVE FUNCTION

Here, our purpose is to obtain an appropriate wave function using the canonical quantization method for a photon emitted from an atom. The approach commonly starts from the interaction of light with matter. In fact, the matter is supposed to be a harmonic polarization field or atomic medium in the canonical quantization method. So, the contributed Hamiltonian is given by:

$$\begin{aligned} H_0 &= \varepsilon_0(E^2 + \omega_k^2.A^2) \\ H_m &= m.\omega_m^2.X^2 + \frac{P^2}{m} \\ H_{\text{int}} &= \alpha.\frac{A.P}{m} \end{aligned} \tag{1}$$

where $H_0$, $H_m$, and $H_{int}$ are, respectively, the incident field, atom's field, and interaction Hamiltonians. Also, $\varepsilon_0$, $\omega_k = 2\pi f_k$, m, $\omega_m = c/\lambda_m$, and $\alpha$ are the free space permittivity, incident angular wave frequency, oscillator mass, matter oscillator angular frequency ($\lambda_m$ is the related wavelength), and interaction coefficient between incident field and atom's field, respectively. Moreover, in (1), **E**, **A**, **X**, and **P** are the electric field, vector potential, position, and momentum operators, respectively. Through defining the annihilation and creation operators, the related Hamiltonians can be re-expressed as:

$$\begin{aligned} H_0 &= \hbar\omega_k(a^+a + 1/2) \\ H_m &= \hbar\omega_m(b^+b + 1/2) \\ H_{\text{int}} &= -\alpha.\frac{i\hbar}{2m}\sqrt{\frac{m\omega_m}{\varepsilon_0\omega_k}}(a^+ + a)(b - b^+) \end{aligned} \tag{2}$$

where ($a^+$, a) and ($b^+$, b) indicate the creation and annihilation operators of the incident field and polarization field, respectively. Also,  is the reduced Planck's constant. Dropping the nonconserving energy terms due to the rotating wave approximation, by considering different modes, the interaction Hamiltonian is re-expressed as:

$$H_{\text{int}} = \frac{i\hbar}{2}\sum_k \sqrt{\frac{\alpha^2}{m\varepsilon_0}.\frac{\omega_m}{\omega_k}}(a_k b^+ e^{-j[\omega_k t - k.r]} - a_k^+ b e^{j[\omega_k t - k.r]}) \tag{3}$$

where the term $\sqrt{(\alpha^2/m/\varepsilon_0)}$ indicates the rate of interaction between the incident field and polarization field. To calculate the emitted photon wave function using $<0|E^+(r,t)|\gamma_0>$, we initially need to examine the time evolution of the state of atoms interacted with the incident field $|\gamma_0>$. The state of the interaction of the incident photons with atoms can be expressed using quantum superposition between the atoms in an excited state with no photonic mode and the state of all photonic mode while the atom is in the ground state as:

$$|\gamma_0(t)> = C_b(t)|b, 0> + \sum_k C_a(t)|a, 1_k> \tag{4}$$

where $C_b$ and $C_a$ are the probability of finding atoms in the excited state |b> with no incident photons and the probability of finding atom in ground state |a> due to the interaction with a photon of mode k, respectively. To make the time evolution of the considered state, one can use the Schrödinger equation as:

$$\begin{aligned} &|\dot{\gamma_0(t)}> \\ &= \frac{-i}{\hbar}H_{\text{int}}|\gamma_0(t)> \rightarrow \dot{C_b(t)}\,|b, 0> + \sum_k \dot{C_a(t)}\,|a, 1_k> \\ &= \sum_k \sqrt{\frac{\alpha^2}{4m\varepsilon_0}.\frac{\omega_m}{\omega_k}}\left\{\sum_k C_a(t)e^{-j[\omega_k t - k.r]}|b, 0> \right. \\ &\qquad \left. -C_b(t)e^{j[\omega_k t - k.r]}|a, 1_k>\right\} \end{aligned} \tag{5}$$

One can re-express (5) as a coupled equation regarding the frequency sweeping:

$$\begin{cases} \dot{C_a(t)} = -\sqrt{\frac{\alpha^2}{4m\varepsilon_0}.\frac{\omega_m}{\omega_k}}.C_b(t)e^{j[(\omega-\omega_k)t - k.r]} \\ \dot{C_b(t)} = \sum_k \sqrt{\frac{\alpha^2}{4m\varepsilon_0}.\frac{\omega_m}{\omega_k}}.C_a(t)e^{-j[(\omega-\omega_k)t - k.r]} \end{cases} \tag{6}$$

Through the integration of each side of the first part of (6) and substituting into the second part, the equation becomes:

$$\dot{C_b(t)} = -\sum_k \frac{\alpha^2}{4m\varepsilon_0}.\frac{\omega_m}{\omega_k}.\int_0^t dt' C_b(t')e^{j(\omega-\omega_k)(t-t')} \tag{7}$$

Since the modes are so closely spread, then one can replace summation with integration in the volume V through which (7) is presented as:

$$\begin{aligned} &\dot{C_b(t)} \\ &= -\frac{2V}{(2\pi)^3}\int dk^3 \left\{\frac{\alpha^2}{4m\varepsilon_0}.\frac{\omega_m}{\omega_k}.\int_0^t dt' C_b(t')e^{j(\omega-\omega_k)(t-t')}\right\} \end{aligned} \tag{8}$$

where $dk^3 = k^2\sin(\theta)dkd\theta d\varphi$. Using $k = \omega_k/c$ and $dk = d\omega_k/c$, and by assuming that $\omega_k$ can be supposed as a constant in the considered bandwidth, (8) can be simplified as:

$$\begin{cases} \dot{C_b(t)} = -\frac{2V}{(2\pi)^3}\int_0^{2\pi} d\varphi \int_0^{\pi} \sin\theta d\theta \int_0^t dt' C_b(t') \\ \qquad \times \left\{\frac{\alpha^2\omega_m}{4m\varepsilon_0}\int_0^{\infty}\frac{\omega_k^2}{c^2}e^{j(\omega-\omega_k)(t-t')}\frac{d\omega_k}{c\omega_k}\right\} \\ \dot{C_b(t)} = -\frac{2V}{(2\pi)^3}.4\pi.\frac{\omega_k}{c^3}.\frac{\alpha^2\omega_m}{4m\varepsilon_0}.\int_0^t dt' C_b(t').\delta(t'-t) \\ \qquad \rightarrow -\frac{2V}{(2\pi)^3}.4\pi.\frac{\omega_k}{c^3}.\frac{\alpha^2\omega_m}{4m\varepsilon_0}C_b(t) \end{cases} \tag{9}$$

From (9), $C_b(t) = \exp[-\Gamma_q^* t/2]$, where $\Gamma_q = (V/4\pi^2)(\omega_k/c^3)(\omega_m \alpha^2/m\varepsilon_0)$. Then, $C_b(t)$ is substituted into the first part of (6), leading to the calculation of $C_a(t)$ as:

$$C_a(t) = -\sqrt{\frac{\alpha^2}{4m\varepsilon_0}.\frac{\omega_m}{\omega_k}}.e^{-jk.r}\int_0^t dt' C_b(t) e^{-j[(\omega-\omega_k)+\frac{\Gamma_q}{2}]t'} \tag{10}$$

So, $C_a(t)$ is expressed in the steady-state condition as:

$$C_a(t) = i\sqrt{\frac{\alpha^2}{4m\varepsilon_0}.\frac{\omega_m}{\omega_k}}.\frac{e^{-jk.r}}{(\omega-\omega_k)+i\frac{\Gamma_q}{2}} \tag{11}$$

Finally, the state of the interaction between the incident photon and polarization field by ignoring $C_b(t)$ effect can be introduced as:

$$|\gamma_0> = i\sum_k \sqrt{\frac{\alpha^2}{4m\varepsilon_0}.\frac{\omega_m}{\omega_k}}.\frac{e^{-jk.r}}{(\omega-\omega_k)+i\frac{\Gamma_q}{2}}|1_k> \tag{12}$$

We are now ready to calculate the emitted photon wave function, $\psi_c(r, t)$, using the canonical quantization method. The related wave function due to the interaction of the incident photon with the polarization field is derived from [9], [12]:

$$\begin{aligned}\Psi_c(r,t) &= <0|E^+(r,t)|\gamma_0> \\ &= <0|E^+(r,t)|i\sum_k \sqrt{\frac{\alpha^2}{4m\varepsilon_0}.\frac{\omega_m}{\omega_k}}.\frac{e^{-jk.r}}{(\omega-\omega_k)+i\frac{\Gamma_q}{2}}|1_k>\end{aligned} \tag{13}$$

where $E^+(r, t)$ is the quantized electric field and can be substituted in (13) to finalize as:

$$\begin{aligned}\Psi_c(r,t) =& <0|i\sum_{k'}\sqrt{\frac{\hbar\omega_{k'}}{2V\varepsilon_0}}e^{-j(\omega_{k'}t-k.r)}a_{k'} \\ & .i\sum_k \sqrt{\frac{\alpha^2}{4m\varepsilon_0}\frac{\omega_m}{\omega_k}}\frac{e^{-jk.r_0}}{(\omega-\omega_k)+i\frac{\Gamma_q}{2}}|1_k>\end{aligned} \tag{14}$$

After some algebraic simplification and using $k = k'$, (14) can be re-expressed as:

$$\Psi_c(r,t) = -\sum_{k'}\sqrt{\frac{\hbar\alpha^2\omega_m}{8V\varepsilon_0^2}}.\frac{e^{-j\omega_k t}e^{jk.(r-r_0)}}{(\omega-\omega_k)+i\frac{\Gamma_q}{2}} \tag{15}$$

By transferring the summation to integral and make some algebraic simplifications, (15) is finally presented as:

$$\begin{aligned}\Psi_c(r,t) &= \frac{-2V}{(2\pi)^3}\int dk^3\sqrt{\frac{\hbar\alpha^2\omega_m}{8V\varepsilon_0^2}}.\frac{e^{-j\omega_k t}e^{jk.(r-r_0)}}{(\omega-\omega_k)+i\frac{\Gamma_q}{2}} \\ &\xrightarrow{k=\frac{\omega}{c},k_0=\frac{\omega_k}{c}} = \frac{-1}{(2\pi)^3}\sqrt{\frac{\hbar\alpha^2\omega_m V}{2\varepsilon_0^2}}\int_{-\infty}^{\infty}k^2dk \\ &\quad .\frac{e^{-j\omega_k t}e^{jk_0.(r-r_0)}}{c[(k-k_0)+i\frac{\Gamma_q}{2c}]}\end{aligned} \tag{16}$$

Using the Residue method, the integral in (16) is solved as:

$$\begin{aligned}\Psi_c(r,t) = \frac{i}{(2\pi)^2}\sqrt{\frac{\hbar\alpha^2\omega_m V}{2\varepsilon_0^2}}\frac{\omega_k^2}{c^3}e^{-j\omega_k t}e^{jk_0.(r-r_0)} \\ \times e^{\frac{-\Gamma_q}{2}[\frac{k_0(r-r_0)}{c}-t]}\end{aligned} \tag{17}$$

Defining $\eta_c = 0.5^*\Gamma_q[k_0'(r - r_0)/c - t]$, (17) is given by:

$$\Psi_c(r,t) = \frac{i}{2(2\pi)^2}\sqrt{\frac{2\hbar\alpha^2\omega_m V}{\varepsilon_0^2}}\frac{\omega_k^2}{c^3}e^{-\eta_c - j\omega_k t}e^{jk_0.(r-r_0)} \tag{18}$$

Thus, one can compare the emitted photon wave function derived for the canonical quantization method in (18) with the wave function derived by the dipole approximation method [12] as:

$$\Psi_d(r,t) = \frac{i}{2(2\pi)^2}\frac{e}{\varepsilon_0}(d_{ab}\bullet\varepsilon_k)\frac{\omega_k^3}{c^3}e^{-\eta_d - j\omega_k t}e^{jk_0.(r-r_0)} \tag{19}$$

where e, $\eta_d$, $d_{ab}$, and $\varepsilon_k$ are the electron charge, excited state decay rate, and dipole moment of transition and incident photon polarization. In fact, $(d_{ab}.\varepsilon_k)$ defines the type of coupling between the incident photons and the dipole operator. It can be easily shown that $\Psi_d(\Delta R,t)$ and $\Psi_c(\Delta R,t)$ have the same unit.

Based on the schematic illustrated in Fig. 1, one can define the radar cross-section for the two different approaches as $\sigma_d = \lim_{r\to\infty} 2\pi r * (I_{sd}/I_0)^2$ and $\sigma_c = \lim_{r\to\infty} 2\pi r * (I_{sc}/I_0)^2$, where $I_{sd}$ and $I_{sc}$ are the scattering photons intensity for the canonical conjugate and dipole approximation methods, respectively. Herein, we want to study the difference between two analysis methods; we need to analyze $\sigma_c/\sigma_d \sim [\Psi_c(\Delta R,t)/\Psi_d(\Delta R,t)]^2$:

$$\begin{aligned}\frac{\Psi_c(r,t)}{\Psi_d(r,t)} &= \left\{\frac{\frac{i}{2(2\pi)^2}\sqrt{\frac{2\hbar\alpha^2\omega_m V}{\varepsilon_0^2}}\frac{\omega_k^2}{c^3}e^{-\eta_c - j\omega_k t}e^{jk_0.(r-r_0)}}{\frac{i}{2(2\pi)^2}\frac{e}{\varepsilon_0}(d_{ab}\bullet\varepsilon_k)\frac{\omega_k^3}{c^3}e^{-\eta_d - j\omega_k t}e^{jk_0.(r-r_0)}}\right\} \\ &= \frac{1}{(d_{ab}\bullet\varepsilon_k)}\sqrt{\frac{2\hbar\alpha^2\omega_m V}{e^2}}\frac{1}{\omega_k}e^{\eta_d-\eta_c}\end{aligned} \tag{20}$$

First of all, one can simply suppose $\eta_d \sim \eta_c$. It is also assumed that the electric dipole momentum $\mathbf{d_{ab}}.\boldsymbol{\varepsilon_k}$ can be considered the same as $\alpha$, which stands for the coupling between the incident and polarization fields in the canonical quantization method. With the listed assumptions, (20) is reduced to:

$$\frac{\Psi_c(r,t)}{\Psi_d(r,t)} \sim \sqrt{\frac{2\hbar V}{e^2}.\frac{\omega_m}{\omega_k^2}} \tag{21}$$

By considering $V = 4\pi r^3/3$, where r is the far-field distance given as $r >= 2D^2/\lambda_k$, and also D is the largest dimension of the scatter. The simulation results are depicted in Fig. 2 for the range of incident wave frequency 1.5 GHz $< f_k <$ 60 GHz, and D $\sim$ 0.1 mm, and r >= 200 nm. The result in Fig. 2 reveals that for the frequency less than 2 GHz, the emitted photons by the canonical quantization method

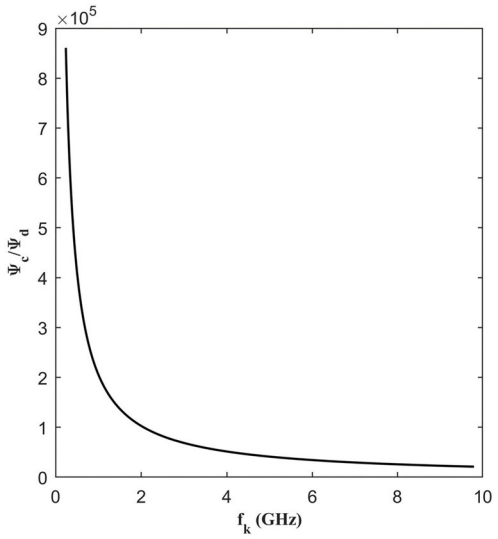


**FIGURE 2.** The comparison between $\Psi_d$ and $\Psi_c$ for $\eta_d \sim \eta_c$ and $\alpha \sim \mathbf{d_{ab}}.\boldsymbol{\varepsilon_k}$.

is much more than the dipole approximation method. It is worthy to note that to calculate $\sigma_c/\sigma_d$, we need to consider the square power of $[\Psi_c(\Delta R,t)/\ \Psi_d(\Delta R,t)]$. By increasing the incident frequency, the ratio of the amplitude $[\Psi_c(\Delta R,t)/\ \Psi_d(\Delta R,t)]$ is dramatically decreased. Nonetheless, the simulated result shows that the emitted photon from the target through the canonical quantization method is approximately $2^*10^5$ times the dipole approximation method at $f_k = 1$GHz. This means that the dipole approximation method ignores some critical points when utilizing the approximation procedure. In other words, the result depicted in Fig. 2 suggests that the radar cross-section main lobe may be enhanced beside the sidelobe.

The RCS sidelobe improvement is fully predicted by QRCS [12], [13], while the latter mentioned methods cannot forecast anything about the main lobe.

Regarding the mentioned points, however, one needs enough details about (20) to thoroughly compare the two different methods. To do so, we focus on time constants by which the atom's excited state is decayed. That is the comparison between $\eta_d$ and $\eta_c$. For better understanding, one can notice the simulation results displayed in Fig. 3. In this figure, to easily compare the results, $\eta_d$ is multiplied by 1000 because $\eta_d$ is much less than $\eta_c$. This figure shows that decay rates derived with the canonical quantization and dipole approximation method show the same behavior at very low frequency. This means that the exponential term in (20) can be ignored at a low frequency. However, by increasing the frequency, $\eta_c$ becomes dominant; This means that the excited state of the atom predicted by the canonical quantization method is sharply decayed at the RF frequency compared to the dipole approximation method. Furthermore, to thoroughly analyze (20), we need to know the behavior of $\exp[\eta_d - \eta_c]$ shown in Fig. 4. It is demonstrated that $\exp(\eta_d - \eta_c)$ is so close to unity, which means that it doesn't have a critical effect on $\Psi_d(\Delta R,t)/\ \Psi_c(\Delta R,t)$, especially in

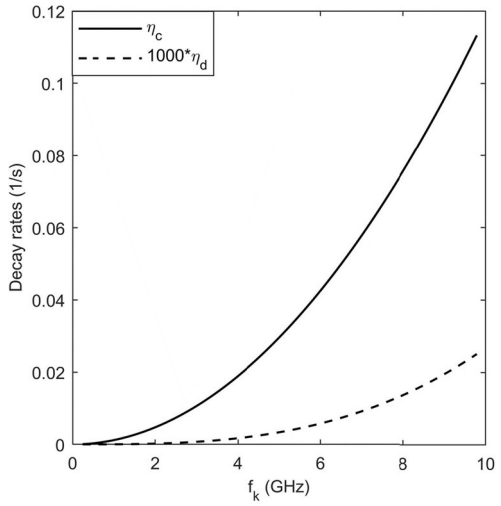


**FIGURE 3.** The comparison between $\eta_d$ and $\eta_c$ for $\alpha = \mathbf{d_{ab}}.\boldsymbol{\varepsilon_k}$.

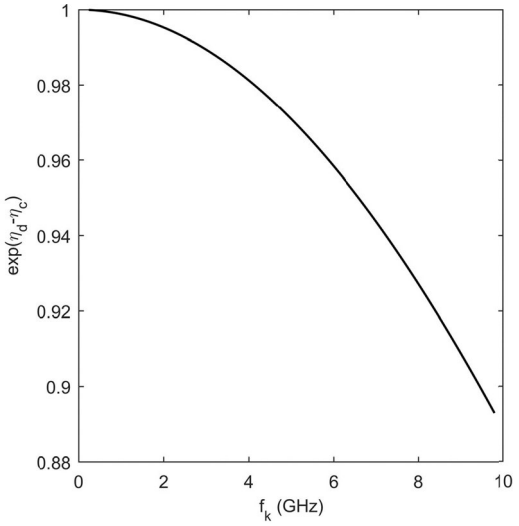


**FIGURE 4.** The change of $\exp[\eta_d - \eta_c]$ vs. frequency for $\alpha = \mathbf{d_{ab}}.\boldsymbol{\varepsilon_k}$.

the range of 0.5∼3 GHz. Thus, the term $\exp[\eta_d - \eta_c]$ can be safely ignored at that mentioned range of frequency.

Nonetheless, the crucial case to compare $\Psi_d(\Delta R,t)$ and $\Psi_c(\Delta R,t)$ is the difference between $\alpha$ and $\mathbf{d_{ab}}.\boldsymbol{\varepsilon_k}$. So, in the following, we want to thoroughly study two terms and investigate $\Psi_c(\Delta R,t)/\ \Psi_d(\Delta R,t)$ in the non-ideal form.

From the semi-classical point of view, $\mathbf{d_{ab}}$ is the electric dipoles of the atom randomly oriented in each direction. To analyze precisely, one can express the atom's electric dipole and photon's polarization vector as:

$$\begin{aligned} \overrightarrow{d_{ab}} &= \overrightarrow{d} \ < \sin\xi\cos\zeta, \sin\xi\sin\zeta, \cos\xi > \\ \overrightarrow{\varepsilon_k} &= < \sin\theta\cos\varphi, \sin\theta\sin\varphi, \cos\theta > \end{aligned} \tag{22}$$

The vectors in (22) are presented in the spherical coordinates in which two different azimuth and elevation angles are defined to distinguish between the atom dipole orientation and the incident photon polarization direction. Operator $d_{ab}$ is the radial component of the dipole operator, which

operates on atom's states. It has generally been considered two different scenarios for the case of $\mathbf{d_{ab}}$. The first scenario assumes that each dipole direction is uniformly distributed, so each atom has the same average value, and one can use mean($|\mathbf{d_{ab}}.\boldsymbol{\varepsilon_k}|^2$) rather than $\sum_{i=1}^{N}|\mathbf{d_{abi}}.\boldsymbol{\varepsilon_{ki}}|^2$. The second scenario is that all of the electric dipoles are oriented in the same direction. That is like immersing an object into a string field. Therefore, the term ($|\mathbf{d_{ab}}.\boldsymbol{\varepsilon_k}|^2$) is the same for all atoms. That means that $\sum_{i=1}^{N}|\mathbf{d_{abi}}.\boldsymbol{\varepsilon_{ki}}|^2 = N^*(|\mathbf{d_{ab}}.\boldsymbol{\varepsilon_k}|^2)$.

For two defined scenarios above, the first one seems to be reasonable for the present application (RCS calculation) in which due to the attenuation of the medium such as atmosphere, the target senses a low-intensity field. Thus, the mean value of the $\mathbf{d_{abi}}.\boldsymbol{\varepsilon_{ki}}$ is considered, which indicates a constant number can define the dipole operator coupling with the photon's polarization. After a short introduction about the dipole momentum, to complete the analysis, we need to express $\alpha$ in terms of the atom's transition momentum. From the dipole approximation method, if one considers the mean value of $\mathbf{d_{abi}}.\boldsymbol{\varepsilon_{ki}}$ as a constant, the atom-field coupling factor is defined as [19]:

$$g_d = \varsigma\frac{E}{\hbar} \tag{23}$$

where E is the electric field, and $\varsigma$ is the atom's transition momentum equal to the mean value of e.($\mathbf{d_{abi}}.\boldsymbol{\varepsilon_{ki}}$). Thus, eigenstates of the atom's state are shifted by $g_d$. It is noteworthy to mention that $\varsigma$ is a characteristic constant of the atom and only depends on the wave function of the electronic states, which are not changed inside the cavity (considering the first scenario). Therefore, $g_d$ is strongly dependent on just an incident field. This is the point we want to relate the canonical quantization method's coupling constant to the dipole approximation method's characteristics constant. From the canonical quantization method, we know that a term $\sqrt{(\alpha^2/m/\varepsilon_0)}$ indicates the rate of interaction between the incident field and the polarization field. Therefore, by substituting the rate of interaction into (23), $\alpha$ can be estimated as:

$$\sqrt{\frac{\alpha^2}{m\varepsilon_0}} = \varsigma\frac{E}{\hbar} \rightarrow \alpha = \varsigma\sqrt{\frac{m\omega_k}{2\hbar V}} \tag{24}$$

where (24) indicates the relationship between $\alpha$ and $\varsigma$. By substituting (24) into (20), one can exactly predict $\Psi_d(\Delta R,t)$ and $\Psi_c(\Delta R,t)$. The results in the non-ideal form are shown in Fig. 5. At a frequency such as 2 GHz, $\Psi_c = 40\Psi_d$, which means that $\sigma_c \sim 1600\sigma_d$. Thus, RCS predicted by the canonical quantization method is greater than the dipole approximation method. Moreover, from this figure, one can clearly understand that the exponential term in (20) has a slight effect in the range of RF frequency.

With the results simulated above, it is shown that RCS calculated by the canonical quantization method significantly differs from the dipole approximation method. That is contributed to the difference in the coupling factor employed by two different methods. Also, from the relationship $\sigma_c/\sigma_d \sim$

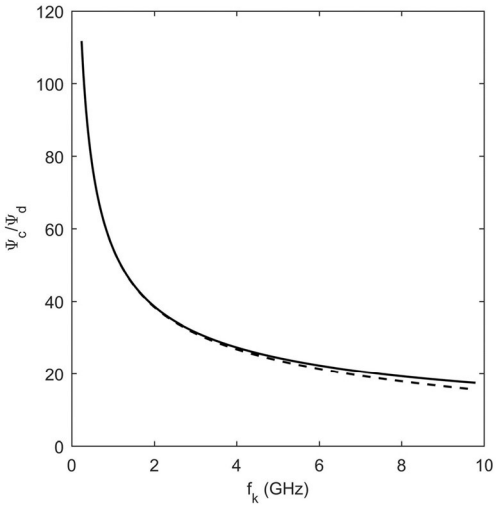


**FIGURE 5.** The comparison between $\Psi_d$ and $\Psi_c$; bold: $\eta_d = \eta_c$, dashed: $\eta_d \neq \eta_c$.

$[\Psi_c(\Delta R,t)/\Psi_d(\Delta R,t)]^2$, one can find that the emitted photons amplitude from the target is the critical factor that RCS is defined based on it. Consequently, from $\Psi_c(\Delta R,t) > \Psi_d(\Delta R,t)$, the comparison $\sigma_c \gg \sigma_d$ is easily deduced, which means that RCS predicted by the canonical quantization method is strongly enhanced. In the following, we want to introduce a new numerical method utilizing a quantum approach to confirm this point.

So far, using full quantum theory, the corresponding formulas are theoretically derived, and results show that the amplitude of photons emitted by the canonical quantization is much greater than the dipole approximation method. In fact, the results show that there is a crucial difference between the canonical quantization method and dipole approximation by which one can infer that the prediction of QRCS may be incomplete. That means that QRCS [9], [12], maybe, cannot predict the main lobe amplitude enhancing as well as sidelobe. In the following, we establish a new method to calculate RCS by merging a quantum approach into the Method of Moment called QMoM. Our purpose is to utilize MoM with the current density operator to compute the scattering field and the related RCS. It is shown that using the current density operator [7], [18] in QMoM gives us some degree of freedom ignored in the classical picture, CRCS, in which the average of the current density has been employed [5]. We want to show by QMoM that using dipole approximation to calculate RCS is not a complete method.

### B. QMoM: USING THE QUANTUM APPROACH IN METHOD OF MOMENT TO CALCULATE RCS

Since an incident field is illuminated on a PEC object, the total field becomes the sum of the incident and scattered fields when the object is exposed. The scattered field includes reflected, diffracted, and surface wave components. To initialize the MoM approach, one commonly uses the Huygens' equivalence principle [20] in which the object is replaced with the same parameter of the outside medium and

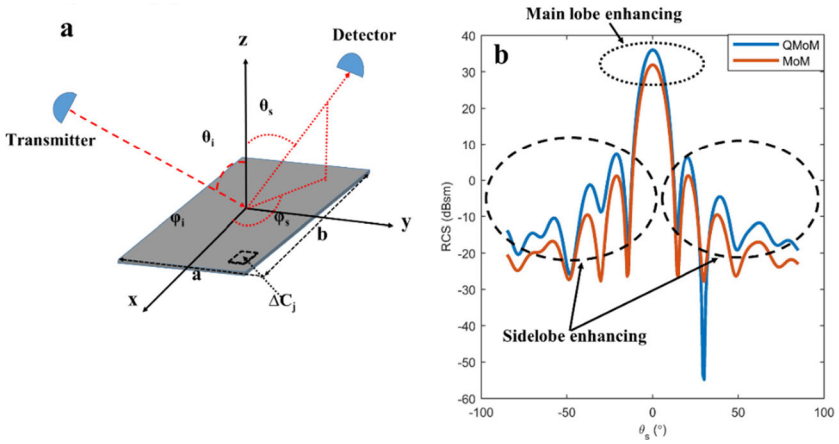


**FIGURE 6.** a) Square plate geometry and the illumination of the microwave photons with angle $\theta_i$, $\varphi_i$ and scattering angle $\theta_s$, $\varphi_s$. $\Delta C_j$ stands $j^{th}$ unit of the segmentation used in MoM; b) QMoM and MoM comparison for the calculation of RCS of 1m * 1m rectangular target illuminated at f = 1.2 GHz and $\theta_i = 0$, $\varphi_s = \varphi_i = 0$.

considers equivalent electric and magnetic current densities on the surface.

Due to the PEC assumption, $M_s = 0$, it is because the tangential component of $E_{tangential}$ equals zero on the surface of PEC. Thus, the scattered fields are just created by $J_s$. Therefore, we focus on the boundary condition on which $E_{tangential} = 0$, then it can be concluded that $\mathbf{n}\times(E^s_{due\ to\ Js} + E^i) = 0$. In the following section, we need to express Maxwell's equations in terms of $E^s$, which involves the integration of $J_s$ that leads to a Fredholm integral equation by which $J_s$ can be solved. The derivation of the QMoM method from classical MoM can be found in detail in Supplementary materials (Appendix A).

From Appendix A, (A9) is the modified version of the classical MoM Fredholm integral presented in (A2), is expressed as:

$$\sum_{j=1}^{N} |C_j|^2 \frac{k\eta}{4} \cdot \frac{e\hbar k}{m} \int_{\Delta C'_j} dl' \left\{ |F_j(r')|^2 H_0^{(2)}(k|r_i - r'|) \right\} = E_z^i(r_i), \quad (25)$$

In this study, we nominate the new version of MoM as QMoM. From (25), one can get N equations for each weight function. Through construction N∗N matrix as $[A]_{nn}[C_j]_{n1} = [bj]_{n1}$, one can find $C_j$ and plugging in $\Phi(r,t) = \sum_{j=1}^{N} C_j F_j(r)$ to calculate the current density. After solving the matrix system for unknown coefficients corresponding to $J_z$ distribution, we can calculate the scattered field using (C1) to analyze the RCS. In the following section, the simulation results are presented.

## III. RESULTS AND DISCUSSIONS

To apply QMoM, we consider a 1m*1m metal square plate illuminated by a microwave wave illustrated in Fig. 6a. Since the aim is to verify the new approach by comparing it with the simulated and published results [5], [12], and [13], for this reason, a simple geometric shape is selected. There are some numerical and theoretical modeling of RCS for a metal square plate [5], [13], [21]. The simulated result in Fig. 6b shows that using QMoM improves the main lobe beside the sidelobe as an important result that can be discussed. This figure shows the difference between MoM and QMoM of calculation of RCS for a square with a dimension of 1m*1m at f = 1.2 GHz and $\theta_i = 0$, $\varphi_s = \varphi_i = 0$. The figure indicates using a dotted circle that the main lobe is enhanced in magnitude as well as the sidelobe, which means that QRCS cannot predict the main lobe improving. Enhancing in magnitude implies the increase of the absolute value of the reflected photons wave function derived in (18). This point is because of the difference between $\Psi_c(\Delta R,t)$ and $\Psi_d(\Delta R,t)$, which are the critical factors in RCS defining. Also, in QMoM, the results strongly contributed to the quantization of the current derived in (C6). In other words, when the current density operator is utilized as expressed in (C6), it means that the imaginary part of the wave function affects the result beside the real part. It is noteworthy to mention that the result illustrated in Fig. 6 is completely comparable with Fig. 5 of [13] and Fig. 4 of [5] in which a rectangular plate 1m * 1m has been incident at 1.2 GHz.

Furthermore, to certify the QMoM and make a comparison with a classical MoM, we have studied the effect of the incident wave frequency, incident angle, and the geometrical shape effects on RCS. We show that all of the results are comparable with the results of published works [5], [13], and [21]. The related results can be found in the Supplementary materials (Appendix B).

## IV. CONCLUSION

In this article, RCS was calculated using the canonical quantization method, which is a more comprehensive theory than the dipole approximation. The main aim was to compare the difference between two quantum-based theories dealing with the RCS calculation. It was shown that there are some similarities between two quantum-based methods at some

specific range of frequencies; nonetheless, it was revealed that there are a few crucial factors that have been ignored in the dipole approximation methods. The main difference between the dipole approximation and canonical quantization method to calculate radar cross-section was issued from the interaction Hamiltonian. In other words, it was the coupling factor that created a significant difference between the two methods.

In this study, RCS was calculated for a system by two different methods with the same conditions. The results revealed that the emitted photons calculated by the canonical quantization method are more than that of dipole approximation. This point severely affected the RCS calculation. To prove this point, we established a new numerical method in which the quantum theory is utilized in MoM to enhance the calculation of RCS rather than QRCS. The idea of the QMoM initiated from this point that using the current density operator rather than the current density average could enhance the results. Thus, using quantum theory, the current density operator was derived and substituted into the MoM approach. The simulated results showed this approach could enhance the sidelobe in the same way with QRCS; interestingly, it also revealed that the main lobe intensity was enhanced. That is contributed to the difference between the current density average used in the classical MoM and the current density operator utilized in the new method as QMoM.

To confirm the QMoM operation accuracy, the effect of some parameters such as frequency, incident angle, and shape changes are considered on RCS calculation. The results revealed full compatibility in accuracy between MoM and QMoM as one could compare the results with the different cited works. As a significant result, it can be mentioned that using dipole approximation to calculate RCS is not a complete method. In other words, although the dipole approximation approach to compute the radar cross-section may improve the calculation accuracy with respect to classical radar cross-section; nonetheless, it is not a perfect method.

## REFERENCES

[1] P. Pouliguen, R. Hemon, C. Bourlier, J. F. Damiens, and J. Saillard, "Analytical formulae for radar cross section of flat plates in near field and normal incidence," *Prog. Electromagn. Res.*, vol. 9, pp. 263–279, 2008.

[2] S. H.-Varmazya and Z. Masouri, "A numerical approach for calculating the radar cross-section of two-dimensional perfect electrically conducting structures," *J. Electromagn. Waves Appl.*, vol. 28, no. 11, pp. 1360–1375, 2014.

[3] C. J. Reddy, M. D. Deshpande, C. R. Cockrell, and F. B. Beck, "Fast RCS computation over a frequency band using method of moments in conjunction with asymptotic waveform evaluation technique," *IEEE Trans. Antennas Propag.*, vol. 46, no. 8, pp. 1229–1233, Aug. 1998.

[4] A. K. Bhattacharyya and D. L. Sengupta, *Radar Cross Section Analysis and Control*. Boston, MA, USA: Artech House 1991.

[5] T. Zhang, H. Zeng, and R. Chen, "Simulation of quantum radar cross section for electrically large targets with GPU," *IEEE Access*, vol. 7, pp. 154260–154267, 2019.

[6] I. Nicolaescu and T. L. Oroian, "Radar cross section," in *Proc. 5th Int. Conf. Telecommun. Modern Satell., Cable Broadcast. Service (TELSIKS)*, 2001, pp. 65–68.

[7] R. R. Krishna, R. M. Krishna, R. G. Krishna, and D. Sekhar, "Radar cross section prediction for different objectives using MATLAB and radar cross section (RCS) reduction," *Int. J. Adv. Res. Comput. Sci. Electron. Eng.*, vol. 1, pp. 67–75, 2012.

[8] P. Blacksmith, R. E. Hiatt, and R. B. Mack, "Introduction to radar cross-section measurements," *Proc. IEEE*, vol. 5, no. 8, pp. 901–920, Aug. 1965.

[9] M. Lanzagorta, *Quantum Radar*. San Rafael, CA, USA: Morgan & Claypool, 2012, doi: 10.2200/S00384ED1V01Y201110QMC005.

[10] A. Salmanogli, D. Gokcen, and H. S. Gecim, "Entanglement of optical and microcavity modes by means of an optoelectronic system," *Phys. Rev. A, Gen. Phys.*, vol. 11, Feb. 2019, Art. no. 024075.

[11] A. Salmanogli, D. Gokcen, and H. Selcuk Gecim, "Entanglement sustainability in quantum radar," *IEEE J. Sel. Topics Quantum Electron.*, vol. 26, no. 6, pp. 1–11, Dec. 2020.

[12] M. J. Brandsema, M. R. Narayanan, and M. Lanzagorta, "Theoretical and computational analysis of the quantum radar cross section for simple geometrical targets," *Quantum Inf. Process.*, vol. 6, p. 32, Dec. 2016.

[13] Ch. Fang, H. Tan, Qi-F. Liu, L. Tao, L. Xiao, Y. Chen, and L. Hua, "The calculation and analysis of the bistatic quantum radar cross section for the typical 2-D plate," *IEEE Photon. J.*, vol. 10, no. 2, Apr. 2018, Art. no. 7500614.

[14] H.-L. Dong, S.-X. Gong, P.-F. Zhang, J. Ma, and B. Zhao, "Fast and accurate analysis of broadband RCS using method of moments with loop-tree basis functions," *IET Microw., Antennas Propag.*, vol. 9, no. 8, pp. 775–780, 2015.

[15] G. K. Carvajal, D. J. Duque, and A. J. Zozaya, "RCS estimation of 3D metallic targets using the moment method and Rao-Wilton-Glisson basis functions," *ACES J.*, vol. 24, no. 5, pp. 487–492, 2009.

[16] E. L. Rumyantsev and P. E. Kunavin, "The quantum mechanical probability density and probability current density operators in the pauli theory," 2017, *arXiv:1708.04193*. [Online]. Available: http://arxiv.org/abs/1708.04193

[17] G. M. Wysin, "Probability current and current operators in quantum mechanics," Lecture, Dept. Phys., Kansas State Univ., Manhattan, KS, USA, Tech. Rep., 2011. [Online]. Available: http://www.phys.ksu.edu/personal/wysin

[18] B. Huttner and S. M. Barnett, "Quantization of the electromagnetic field in dielectrics," *Phys. Rev. A, Gen. Phys.*, vol. 46, p. 4306, Oct. 1992.

[19] G. Rempe, "Atoms in an optical cavity: Quantum electrodynamics in confined space," *Contemp. Phys.*, vol. 34, no. 3, pp. 119–129, 1993.

[20] W. C. Chew and C.-C. Lu, "The use of Huygens' equivalence principle for solving the volume integral equation of scattering," *IEEE Trans. Antennas Propag.*, vol. 41, no. 7, pp. 897–904, Jul. 1993.

[21] C. Fang, "The simulation and analysis of quantum radar cross section for three-dimensional convex targets," *IEEE Photon. J.*, vol. 10, no. 1, pp. 1–8, Feb. 2018.

**AHMAD SALMANOGLI** received the B.S. and M.Sc. degrees in electrical engineering from Tabriz University. He is currently pursuing the Ph.D. degree in electrical engineering with Hacettepe University. He has been working as a Research Assistant with Çankaya University since 2018. His research interests include quantum electronics, quantum plasmonic, plasmonic-photonic engineering, quantum optics, and plasmonic-based nanosensor.

**DINCER GOKCEN** (Member, IEEE) received the B.S. degree in electrical engineering from Yıldız Technical University, in 2005, and the Ph.D. degree in electrical engineering from the University of Houston, in 2010. He has been with the National Institute of Standards and Technology, GlobalFoundries, and Aselsan, before joining Hacettepe University as a Faculty Member in 2016. His research interests include nanofabrication, semiconductor process engineering technologies, quantum devices, and sensors.